

Modified Pyridine-Bis(imine) Iron and Cobalt Complexes: Synthesis, Structure, and Ethylene Polymerization Study

Frédéric Pelascini,^[a,b] Marcel Wesolek,^{*[b]} Frédéric Peruch,^{*[a]} and Pierre J. Lutz^[a]

Keywords: N ligands / Iron / Cobalt / Ethylene / Polymerization

In this paper, we describe the synthesis of two new pyridine-bis(imine)s [4-chloro-2,6-bis[1-(2,6-diisopropylphenylimino)ethyl]pyridine and 2,6-bis[1-(2,6-dimethylcyclohexylimino)ethyl]pyridine] and their complexation with iron and cobalt dichloride. The solid-state structure of the iron complexes was solved and found to be very close to catalysts already described by Brookhart and Gibson. Their ability to polymerize ethylene was investigated after activation with MAO. It was thus shown that the substitution of the pyridine ring of

the ligand is unfavorable: their catalytic activity is rather low. The replacement of the aromatic rings on the imine functions by dimethylcyclohexyl rings resulted in a complete loss of activity of the iron complex for oligomerization and polymerization of ethylene. With the cobalt analog, polymerization of ethylene could be achieved under the same conditions.

(© Wiley-VCH Verlag GmbH & Co. KGaA, 69451 Weinheim, Germany, 2006)

Introduction

In 1998, Brookhart and Gibson simultaneously described the synthesis of very active pyridine-bis(imine) iron- or cobalt-based catalysts for the oligomerization or the polymerization of ethylene.^[1–3] When the substituents on the ligand were bulky enough, they were found to be extremely efficient for the synthesis of linear polyethylenes. Many modifications of these ligands have already been described, but it was almost always the R¹–R⁵ (Figure 1) groups that were modified; some reviews are listed with the most recent of these references.^[4–17] So far, less work has been done on other types of modifications (imine functions replaced by amine functions, aryl rings replaced by amines or pyrrolyl rings, pyridine ring replaced by thiophene or furan ring, and so forth).^[18–23] In this paper, we report new kinds of modifications. We focus more specifically on the electronic factors through the synthesis of two new types of pyridine-bis(imine) ligands. With ligand **1**, the presence of the chlorine group in the *para* position of the pyridine ring in the well-known 2,6-bis[1-(2,6-diisopropylphenylimino)ethyl]pyridine ligand (R¹ = R⁵ = isopropyl) led us to study the effect of the electronic-withdrawing chlorine group. For ligand **2**, the replacement of the aryl groups by aliphatic rings of another well-known ligand, 2,6-bis[1-(2,6-dimethylphenylimino)ethyl]pyridine (R¹ = R⁵ =

methyl), was performed. The iron and cobalt complexes, once synthesized, were activated with methylaluminumoxane (MAO) and tested for the polymerization of ethylene.

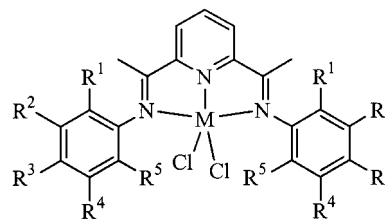


Figure 1. Pyridine-bis(imine) iron or cobalt complexes.

Results and Discussion

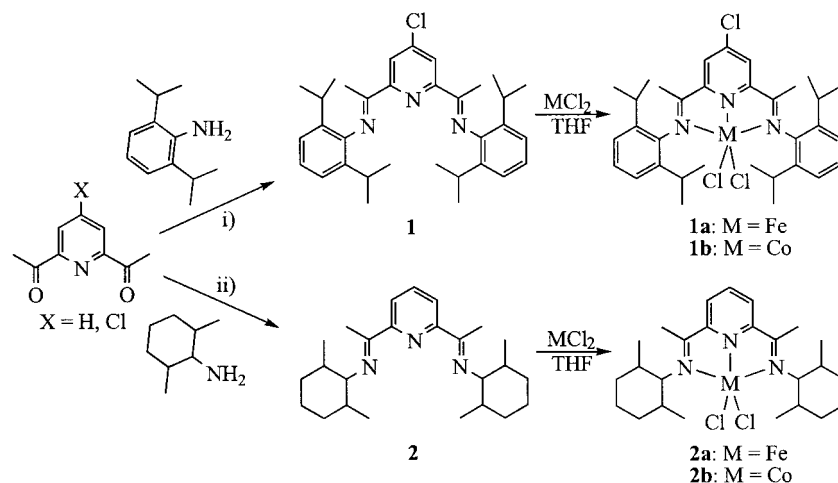
Synthesis and Characterization of Ligands

4-Chloro-2,6-bis[1-(2,6-diisopropylphenylimino)ethyl]pyridine (**1**) was synthesized according to already published procedures for the synthesis of pyridine-bis(imine).^[1,2] The reaction is a condensation between 2,6-diacetyl-4-chloropyridine (synthesis described by Constable^[24]) and 2,6-diisopropylaniline (Scheme 1, i). The yellow product was isolated and characterized by elemental analysis, and ¹H and ¹³C NMR spectroscopy.

Concerning the synthesis of 2,6-bis[1-(2,6-dimethylcyclohexylimino)ethyl]pyridine (**2**), the same procedure was followed but the substituted aniline was replaced by the corresponding cyclohexylamine to yield aliphatic-substituted imines (Scheme 1, ii). Besides, substituted cycloalkanes exhibit several stereoisomers. In the case of 2,6-dimethylcyclohexylamine, three different stereoisomers can be identified: the

[a] Institut Charles Sadron (UPR CNRS 22), 6 rue Boussingault, B. P. 40016, 67083 Strasbourg Cedex, France

[b] Laboratoire de Chimie des Métaux de Transition et de Catalyse (LC3-UMR CNRS 7177), Institut Le Bel, 4 rue Blaise Pascal, 67070 Strasbourg Cedex, France
E-mail: peruch@enscpb.fr
wesolek@chimie.u-strasbg.fr



Scheme 1. Synthesis of ligands **1**, **2all-cis**, **2all-trans** and complexes **1a**, **1b**, **2a**, **2b**.

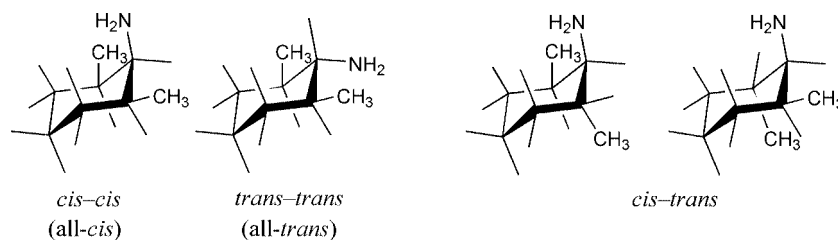


Figure 2. Most stable conformers for each stereoisomer of 2,6-dimethylcyclohexylamine.

cis-cis (all-*cis*), the *trans-trans* (all-*trans*), and the *cis-trans* one (Figure 2). It was decided to use only the pure all-*trans* and all-*cis* amines. After double condensation with diacetyl pyridine, these two products will give few conformers compared to the *cis-trans* one. Indeed, in the case of the *cis-trans* amine, the final pyridine-bis(imine) would probably be a mixture of isomers. Moreover, thanks to a thorough conformational analysis, it was shown that each stereoisomer had several conformers of different stabilization energy. For the all-*cis* and all-*trans* amines the most stable conformer is the one where the two methyl groups are in the equatorial position, thus minimizing steric repulsion. For the all-*cis* amine the amino group takes the axial position and for the all-*trans* amine the same group is in an equatorial position. Thus, normally only one conformer will be obtained for each selected amine. Condensation was carried out under ethanol reflux, with a slight excess of amine and some drops of acetic acid.

Both ligands based on the amine, hereafter named **2all-cis** and **2all-trans**, were characterized by elemental analysis, and ^1H and ^{13}C NMR spectroscopy. In order to better allot the resonance peaks, a COSY spectrum was recorded. It was thus established that the molecule is in a blocked configuration at ambient temperature. Indeed, in the case of unsubstituted cyclohexane, it is known that there is a difference of 0.5 ppm between the chemical shifts of the axial and equatorial protons only at low temperature, when the exchange of cycle is slow compared to the timescale of the NMR spectroscopy. In our case, at ambient temperature,

the conformational exchange is slow; we observe a difference of 0.3 ppm between the axial and equatorial protons, the equatorial protons being the most strongly shielded.

The attribution of the multiplet between 1.0 and 1.9 ppm was possible thanks to a 2D experiment (^1H - ^{13}C). Three broad multiplets that integrate respectively for 10, 2, and 4 protons can be distinguished. One of the main differences between the two NMR spectra is the peak corresponding to the proton of the cycle carried by the carbon linked to the nitrogen atom of the imine function, whose chemical shift changes from 2.9 ppm for the **2all-trans** system to 3.7 ppm for the **2all-cis** system. Moreover, the coupling constant for the triplet goes from 9.3 Hz to 2.2 Hz. This difference may be easily explained with the Karplus and Conroy

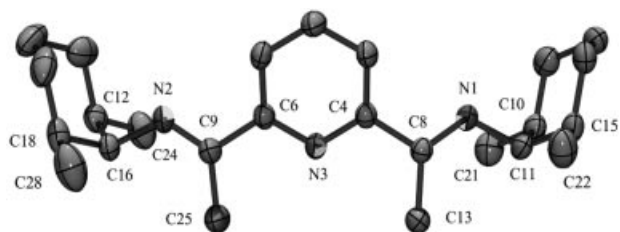


Figure 3. An ORTEP view of the crystal structure of **2all-cis**. Selected bond lengths [Å] and angles [°]: C(6)–C(9) 1.500(2), C(9)–N(2) 1.270(2), N(2)–C(16) 1.465(2), C(18)–C(28) 1.530(3), C(12)–C(24) 1.523(3), C(9)–N(2)–C(16) 121.85(15), N(2)–C(9)–C(25) 126.92(16), C(16)–C(18)–C(28) 111.60(16), C(18)–C(16)–C(12) 110.92(14).

equation. Indeed, ${}^3J_{180^\circ}$ coupling constants are always strictly higher than ${}^3J_{60^\circ}$ ones.

The X-ray structure of the ligand **2all-cis** has been determined to complete the characterization and is represented in Figure 3. Only one conformer is observed, as expected.

Synthesis and Characterization of Complexes

Synthesis and Structure of Iron and Cobalt Complexes with 4-Chloro-2,6-bis[1-(2,6-diisopropylphenylimino)ethyl]pyridine (1a and 1b)

The complexes were obtained from a stoichiometric reaction between the ligand and a suspension of anhydrous FeCl_2 or CoCl_2 in THF at room temperature. In order to recover the complexes, the solution was concentrated and hexane was added to the reaction medium. The iron complex was isolated with a yield of 83% as a blue-green powder. The cobalt complex was isolated with a yield of 81% as a green powder. The isolated complexes were paramagnetic (according to ${}^1\text{H}$ NMR indicating chemical shifts from -40 to 170 ppm) and were characterized by elemental analysis, infrared and X-ray analysis (iron complex only). The elemental analysis results were in agreement with the formula LMCl_2 .

Recrystallization of the iron complex redissolved in diethyl ether yields crystals suitable for X-ray analysis. In the solid state (Figure 4), the geometry of the metal center can be considered as distorted square-pyramidal. One of the chlorine atoms occupies the apical position, with an almost right angle with the iron and nitrogen of the pyridine [$\text{N}(1)(2)(3)\text{-Fe-Cl}(2)$ ranging from 89.3° to 102.5°], whereas the second occupies one of the bases of the formed square. The apical bond seems to be the weaker, as the length of the Fe-Cl bond goes from 2.305 \AA for the apical position to 2.247 \AA for the longitudinal one. This is normally expected for that geometry. The iron atom is slightly above the base of the pyramid [$\text{N}(3)\text{-Fe-N}(1) = 139.2^\circ$]. Predictably, the phenyl groups linked to the imine functions are almost perpendicular to the plane formed by the nitrogen atoms, although there is a slight deformation of the molecule, one of the phenyl groups having a dihedral angle of 94.7° and the other 85.1° .

We can examine the effect of the chlorine atom in the *para* position of the pyridine ring by comparing the lengths of the various bonds with X-ray data of the equivalent nonchlorinated iron complex.^[2] The molecule is asymmetric in the solid state, one of the $\text{Fe-N}_{\text{imine}}$ bonds measuring 2.244 \AA and the other 2.212 \AA . This is probably due to the presence of a molecule of Et_2O in the lattice, but the average value is $2.228(9) \text{ \AA}$, very close to the average value $2.224(9) \text{ \AA}$ for the unsubstituted complex where the lengths of these same bonds are almost identical (in this case half a water molecule is present in the lattice). The decrease in length of the Fe-N_{py} bond for the chlorinated ligand (2.080 instead of 2.091 \AA) can be explained by the fact that the chlorine on the pyridine group enhances the π back donation of the iron to the pyridine group. Another expected

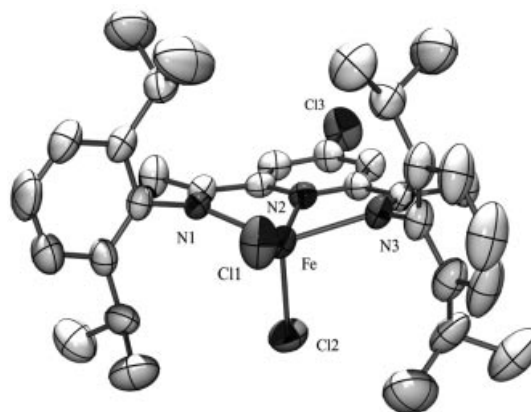


Figure 4. An ORTEP view of the crystal structure of **1a**. Selected bond lengths [\AA] and angles [$^\circ$] for the subunit Fe1: $\text{Fe1-N}(1)$ $2.213(4)$, $\text{Fe1-N}(2)$ $2.080(3)$, $\text{Fe1-N}(3)$ $2.243(4)$, $\text{Fe1-Cl}(1)$ $2.247(1)$, $\text{Fe1-Cl}(2)$ $2.305(2)$, $\text{Cl}(1)\text{-Fe1-N}(1)$ $100.8(1)$, $\text{Cl}(1)\text{-Fe1-N}(2)$ $151.1(1)$, $\text{Cl}(1)\text{-Fe1-N}(3)$ $97.2(1)$, $\text{Cl}(2)\text{-Fe1-N}(1)$ $100.0(1)$, $\text{Cl}(2)\text{-Fe1-N}(2)$ $89.3(1)$, $\text{Cl}(2)\text{-Fe1-N}(3)$ $102.5(1)$, $\text{Cl}(1)\text{-Fe1-Cl}(2)$ $119.55(7)$, $\text{N}(1)\text{-Fe1-N}(2)$ $73.7(1)$, $\text{N}(1)\text{-Fe1-N}(3)$ $139.2(1)$, $\text{N}(2)\text{-Fe1-N}(3)$ $72.9(1)$.

difference is the reduction of the length of the $\text{Fe-Cl}(1)$ bond *trans* to the pyridine group (2.247 instead of 2.263 \AA), while the angle $\text{N}(2)\text{-Fe-Cl}(1)$ where the chlorine and the nitrogen are *trans* to the basal plane varies from 147.9 to 151.1° (for the chlorinated ligand). The apical iron chlorine bond varies from 2.305 (for the chlorinated ligand) to 2.317 \AA , in agreement with the expected electronic effect of the chlorine on the *para* position on the pyridine, that is a decrease of the electronic density on the iron atom. Nevertheless, the solid-state structures of the chlorinated and the nonchlorinated complexes are very close. Besides, as we will see in the structure of $\{2,6\text{-bis}[1\text{-}(2,6\text{-dimethylcyclohexylimino)ethyl]pyridine}\}$ iron dichloride (**2a**), the crystal packing causes little difference in the structure.

Synthesis and Structure of Iron and Cobalt Complexes with 2,6-Bis[1-(2,6-dimethylcyclohexylimino)ethyl]pyridine (2a and 2b)

With the ligand **2all-cis**, no iron or cobalt complexes could be isolated. Indeed, during the reaction between iron chloride and the ligand in THF at ambient temperature, the solution became slightly pink, but no precipitation was observed, even after 24 h. The addition of hexane or diethyl ether did not lead to the precipitation of the complex. Evaporation of solvents to dryness yielded a pink powder. IR results prompted us to think that no complexation occurred, as free FeCl_2 and free ligand were detected. Similar observations were made when the reaction was run at 50°C . Thus, the stoichiometric reaction between the ligand **2all-cis** and the metal chloride did not lead to the formation of the expected complex of formula LMCl_2 . We first made the assumption that a steric factor could be the cause of this nonreactivity, but an X-ray of the free ligand shown in Figure 3 does not confirm this hypothesis.

On the contrary, the addition of 1 equiv. of the ligand **2all-trans** to 1 equiv. of metal chloride in THF at room

temperature led to the formation of the desired complex in good yield (75% for LFeCl_2 and 65% for LCoCl_2). Crystals suitable for X-ray analysis were obtained by slow crystallization in THF. The X-ray crystal structure contains two independent sets of iron complexes, Fe1 and Fe2, with slightly different angles and distances (Figure 5, Table 1).

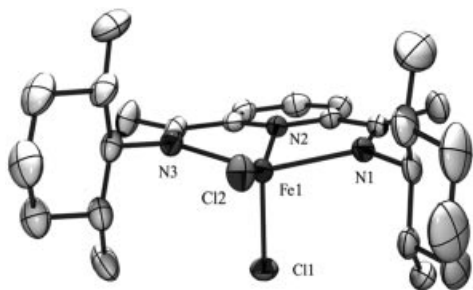


Figure 5. An ORTEP view of the crystal structure of **2a all-trans**. Only one of the two distinct units is represented. The differences in lengths and angles are shown in Table 1.

Table 1. Selected bond lengths [Å] and angles [°] of the two subunits Fe1 and Fe2 for the complex **2a all-trans**.

Bond lengths [Å]			
Fe1–N(1)	2.286(4)	Fe2–N(6)	2.318(4)
Fe1–N(2)	2.087(4)	Fe2–N(5)	2.091(4)
Fe1–N(3)	2.295(4)	Fe2–N(4)	2.308(4)
Fe1–Cl(1)	2.349(1)	Fe2–Cl(3)	2.329(2)
Fe1–Cl(2)	2.279(1)	Fe2–Cl(4)	2.286(1)
Bond angles [°]			
Cl(1)–Fe1–N(1)	97.9(1)	Cl(3)–Fe2–N(6)	95.9(1)
Cl(1)–Fe1–N(2)	91.8(1)	Cl(3)–Fe2–N(5)	95.1(1)
Cl(1)–Fe1–N(3)	95.1(1)	Cl(3)–Fe2–N(4)	102.0(1)
Cl(2)–Fe1–N(1)	103.2(1)	Cl(4)–Fe2–N(6)	102.2(1)
Cl(2)–Fe1–N(2)	153.4(1)	Cl(4)–Fe2–N(5)	155.4(1)
Cl(2)–Fe1–N(3)	101.0(1)	Cl(4)–Fe2–N(6)	102.2(1)
Cl(1)–Fe1–Cl(2)	114.7(1)	Cl(3)–Fe2–Cl(4)	109.4(1)
N(1)–Fe1–N(2)	73.7(2)	N(5)–Fe2–N(6)	72.8(2)
N(1)–Fe1–N(3)	144.5(1)	N(4)–Fe2–N(6)	142.7(2)
N(2)–Fe1–N(3)	73.0(2)	N(4)–Fe2–N(5)	73.2(2)

As in the complexes with an aryl group on the imine functions, the geometry of the metal center can be considered as distorted square-pyramidal, with one of the chlorine atoms occupying the apical position, with an almost 90-degree angle with the iron and the nitrogen atoms: N(1)(2)(3)–Fe1–Cl(1) ranging from 91.8° to 97.9° and N(4)(5)(6)–Fe2–Cl(3) ranging from 95.1° to 102.0°. The average apical Fe–Cl bond (2.35 Å) is longer than the

average equatorial one (2.28 Å), as expected from this type of geometry. It is noticeable that these lengths are higher than for complexes bearing fully aromatic ligands. This seems to indicate that the electronic density on the iron becomes higher. The iron atom is slightly above the base of the pyramid: N(3)–Fe–N(1) 144.5°, which is close to the value found for the aromatic trimethyl analog described by Gibson et al.,^[4] where the value is 145.5°. For comparison, in complex **1a** the angle is 139.2°.

The distances between the iron and both imines are almost identical (average 2.29 Å for Fe1 and 2.31 Å for Fe2). These bonds are a bit longer than for the complex with the 2,4,6-trimethyl aryl substituent^[4] (average 2.27 Å), revealing the electronic effect generated by the replacement of an aryl by a cyclohexyl group. Besides, the Fe–N_{py} bond length with an average of 2.09 Å in complex **2a** is shorter than for the aryl analog, where the value is 2.11 Å. The angle N–Fe–Cl where the nitrogen and the chlorine atom are *trans* to the basal plane is somewhat greater, with an average value of 154.4° in complex **2a** compared to 131.3° in the aryl one.^[4]

Although the cyclohexyl groups are not planar and adopt a chair conformation with the two methyl substituents and the imine in the equatorial position, they are almost perpendicular to the plane of the square base, like aryl groups (dihedral angles: 117.1° and 111.8°). The average distance between the iron atom and the methyl substituents is about 4.3 Å, as already observed for the equivalent aromatic systems.

Ethylene Polymerization with Complexes **1a**, **1b**, **2a**, and **2b** Activated with MAO

All the complexes were activated with methylaluminoxane and tested for the polymerization of ethylene. The results are summarized in Table 2 together with the experimental conditions.

With complexes **1a** and **1b**, polyethylene was produced with the same activity for the two metals, whereas, iron complexes generally present a higher catalytic activity than their cobalt analogs. This result might be due to faster deactivation processes of **1a** versus **1b**. The activities were compared with those observed for the nonchlorinated pyridine complexes (*di*PrFe and *di*PrCo). As indicated in Table 2, the presence of the chlorine atom in the *para* position of the pyridine decreases the catalytic activity, from 2220

Table 2. Ethylene polymerization with iron and cobalt complexes/MAO.

Catalyst ^[a]	Yield [g]	Activity [g·mmol ⁻¹ ·h ⁻¹ ·bar ⁻¹]	Productivity (g _{PE} /g _{Cat.})	M_n ^[b] [g·mol ⁻¹]	M_w ^[b] [g·mol ⁻¹]	MMD ^[c]	T_m ^[d] [°C]	χ ^[d]
1a	1.9	810	295	800	35000	44	97; 136	0.82
<i>di</i> Pr-Fe	5.5	2220	904	2200	48000	22	119; 136	0.82
1b	1.9	810	294	6400	29000	4	135	0.82
<i>di</i> Pr-Co	3.4	1410	556	7000	30000	4	137	0.84

[a] Catalyst: 10 μmol; [Al]/[Met] = 400; P_{Et} = 1 bar; T = 35 °C; t = 15 min; toluene (40 mL). [b] Average molar masses measured by High Temperature Size Exclusion Chromatography in 1,2,4-trichlorobenzene at 150 °C with RI and viscosimetry detection. [c] Molar mass distribution. [d] Melting temperature and crystallinity rate measured by DSC.

810 g·mmol⁻¹·h⁻¹·bar⁻¹ for the iron complexes and from 1410 to 810 g·mmol⁻¹·h⁻¹·bar⁻¹ for the cobalt one. It was thought that slightly decreasing the electronic density on the metal would render the interaction with the incoming ethylene more favorable and then would enhance the catalytic activity.

Actually, this is not what happens because lowering the electronic density on the metal simultaneously disfavors the π back donation of the metal to the incoming ethylene. Bennett did not observe significant falls of activity with a cobalt complex substituted by a trifluoromethyl group in the *para* position of the pyridine ring, but experimental conditions were not comparable.^[25] As the decrease in the catalytic activity cannot be explained by the small differences in the structures of the chlorinated and the nonchlorinated complex, the possible interaction of the chlorine atom present on the pyridine with MAO, used in a large excess, was studied. To do this we have observed by ¹H NMR the chemical shifts of chlorobenzene (to mimic the ligand, this one would coordinate first with the nitrogen groups) in deuterated toluene after addition of a quantity of MAO similar to that used in the polymerization experiment. No significant chemical shifts have been observed, which means that there is probably no interaction between the chlorine atom and the TMA present in the MAO, or the MAO itself. Eventually, the loss of activity observed for the chlorinated complexes could be attributed to the lack of stability of the complex. Indeed, as can be seen on the ¹H NMR spectrum of the complex (Figure 6), a great amount of decomposition product appeared within 20 min; this quantity increases with time. The decomposition process has not been studied in detail.

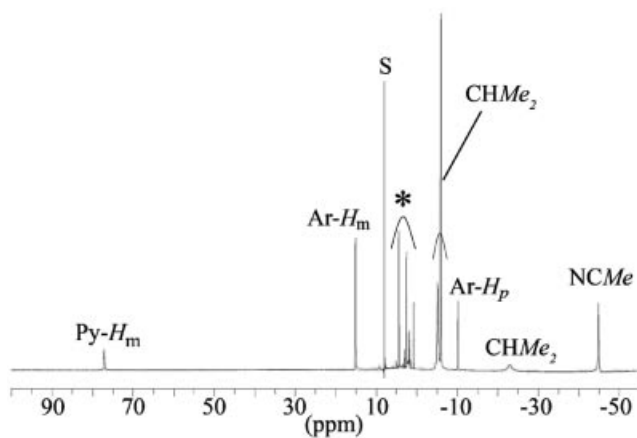


Figure 6. ¹H NMR spectrum of complex **1a**. The peaks of the decomposition product are marked with * (300 MHz, 293 K, CDCl₃).

With the iron complex **2a** no polymers or oligomers have been detected. However, with the cobalt complex **2b** polymers are obtained (no oligomers could be detected by GC). Bianchini obtained oligomers with dissymmetric pyridine-bis(imine) ligands [the imine substituents being an aryl group and a (cyclo)alkyl group].^[21] The proton NMR spectra of the iron complex (Figure 7, a) reveals that almost all the peaks are in the region from -8 to 11 ppm; only the

peaks attributed to the protons on the pyridine are strongly shifted. Although the spectrum was obtained with a large window, from -55 to 250 ppm, some of the protons of the complex cannot be observed, probably because they are too large. Indeed the integration gives 35 protons instead of the 39 expected. An NMR study at low temperature, down to -90 °C, does not reveal new peaks. On the contrary, the broad peak at -11 ppm broadens even further at -70 °C and is invisible at -90 °C.

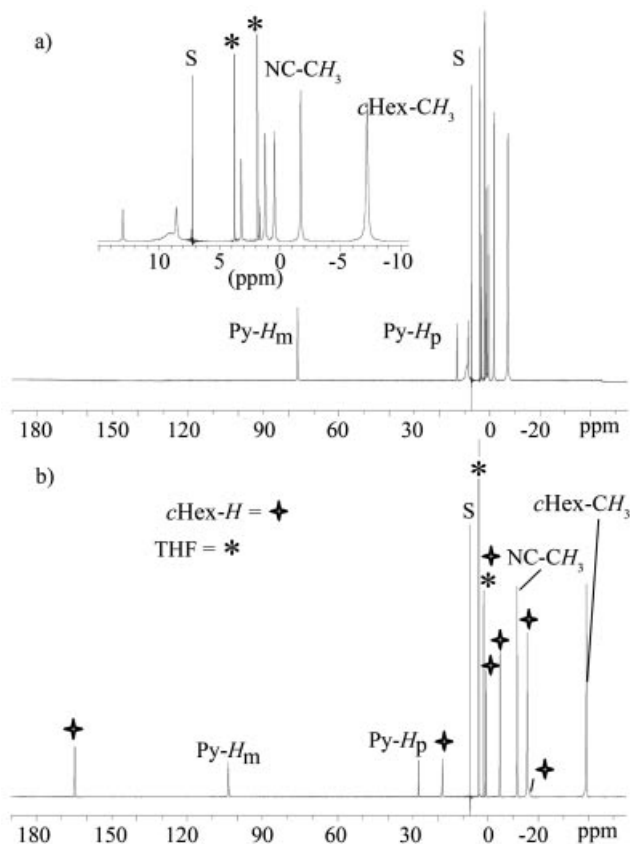


Figure 7. (a) ¹H NMR spectrum of the iron complex **2a** containing THF marked with *; all the other nonmarked peaks are due to the protons on the cyclohexyl group. (b) ¹H NMR spectrum of the cobalt complex **2b** containing THF marked with * (300 MHz, 293 K, CDCl₃).

All the spectra were recorded with pure crystals that contained THF of crystallization; this is the reason two relatively intense peaks of free THF can always be seen in the spectra. In the case of the cobalt complex the proton NMR shows us more important paramagnetic shift: the peaks are in the range -40 to 166 ppm (Figure 7, b). The integration of the peaks corresponds to what is expected.

These observations and the fact that there is a marked difference in the reactivity between the iron and the cobalt complexes bearing the same ligands prompted us to think that the ligand is in some way hemilabile in the case of iron.

The complete loss of activity can then be explained by the assumption that the addition of MAO can hinder the return of the imine group to the iron. On the contrary, for

the cobalt complex **2b**, the spectrum of which is shown in Figure 7 (b), polymerization of ethylene is observed in the presence of MAO. Under 4 bar of ethylene and after 3 h, 150 mg of polyethylene was isolated. We will not go into more detail, as the subject is currently under investigation.

The polymers obtained with **1a** and **1b** were analyzed by ^1H NMR, DSC, and HT SEC. ^1H NMR spectra of polyethylenes ($\text{C}_2\text{D}_2\text{Cl}_4$, 130 °C) present a main peak at 1.3 ppm due to CH_2 groups, and a small one at 0.9 ppm due to CH_3 groups coming from chain ends or branching. Nevertheless, the intensity of the peak at 0.9 ppm is too small to allow reliable integration.

The results of SEC measurements are presented in Table 2. The chlorine atom seems to have no influence on the molar masses or the molar mass distributions when cobalt is employed. For the iron complexes, broad (even bimodal) molar mass distributions were obtained. It is now well established that this is due to transfer to aluminum (TMA present in MAO). It was nevertheless a bit surprising to get such broad distributions, as to avoid this transfer, the MAO we employed had most of its TMA removed by evaporation (5 mol-% residual TMA instead of 30 mol-% in commercial MAO). For cobalt complexes, molar mass distributions were much lower, because these catalytic systems are less sensitive towards transfer to aluminum.

The results of DSC measurements are also presented in Table 2. Like for SEC measurements, no huge differences were observed for the chlorinated and nonchlorinated ligands. The chlorine atom seems to have almost no influence on the melting temperatures and on the crystallinity rate. For all polyethylenes, the crystallinity rate (>0.8) is consistent with highly linear polymers. Polyethylenes obtained with the iron complexes exhibit two melting temperatures corresponding probably to two populations of polymers of different molar masses observed by HT SEC. With the cobalt complexes, only one melting temperature, very close to the one measured for highly linear polyethylene, was observed.

Conclusion

In summary, two new pyridine-bis(imine)s were synthesized, by substituting the pyridine ring, or by replacing the aryl groups linked to the imine functions by an aliphatic ring. These ligands were complexed with iron and cobalt dichloride and two of these four new complexes were characterized by X-ray analysis. All the complexes were tested in the presence of MAO for the polymerization of ethylene. The introduction of a chlorine atom onto the pyridine ring was unfavorable; indeed the catalytic activity decreases compared to the unsubstituted ligand. For the other ligand two different results were observed. In the case of the iron complex, the loss of aromaticity led to a complete loss of catalytic activity towards ethylene polymerization and oligomerization. On the other hand, for the cobalt system, polyethylene could be obtained.

Experimental Section

General Considerations

Anhydrous FeCl_2 and CoCl_2 , diacetylpyridine, chelidamic acid, thionyl chloride, Meldrum's acid, and 2,6-diisopropylaniline (all purchased from Aldrich) were used as received. 2,6-Dimethylcyclohexylamine was kindly provided by BASF AG. Methylaluminoxane (MAO) was purchased from Aldrich as a 10 wt.-% solution in toluene. Toluene and most of the trimethylaluminum (TMA) were removed under vacuum to yield a white powder, still containing 5 mol-% of TMA. Tetrahydrofuran, hexane, and toluene were distilled from sodium benzophenone ketyl. All complex syntheses were performed in a Jacomex glovebox or under thoroughly purified argon using a standard Schlenk technique. 2,6-Diacetyl-4-chloropyridine was prepared according to an already published procedure.^[24]

Characterization

^1H and ^{13}C NMR spectra were recorded with a Bruker Avance-300 apparatus (300 MHz) at room temperature. IR spectra were recorded with a Perkin-Elmer 1600 FTIR spectrometer. Molar masses were measured by Size Exclusion Chromatography using an Alliance GPCV 2000 Permeation Chromatograph equipped with a differential refractive index detector and a viscosimeter in 1,2,4-trichlorobenzene (150 °C) using two Styragel HT 6E and one HT 2 columns. DSC measurements were performed with a Perkin-Elmer DSC4 or DSC7, with a heating rate of 10 °C·min⁻¹.

Synthesis of Ligands

4-Chloro-2,6-bis[1-(2,6-diisopropylphenylimino)ethyl]pyridine (1): 2,6-Diacetyl-4-chloropyridine (0.5 g, 2.5 mmol), 2,6-diisopropylaniline (0.98 g, 5.5 mmol), and a small amount of *p*-toluenesulfonic acid were poured into a three-necked round-bottomed flask containing toluene (50 mL). The solution was refluxed for 24 h with a Dean-Stark trap. After lowering the temperature, the toluene was removed under vacuum to yield a brownish oil. The addition of hexane (20 mL) led to a yellow solution and a brown solid. After filtration and drying, a yellow solid was recovered (0.94 g, yield 72%). ^1H NMR (300 MHz, CDCl_3 , 293 K): δ = 8.48 (s, 2 H, py- H_m), 7.22–7.09 (m, 6 H, Ar- H), 2.74 (sept, $^3J_{\text{H,H}}$ = 6.9 Hz, 4 H, CHMe₂), 2.25 (s, 6 H, N=C-Me), 1.17 (d, $^3J_{\text{H,H}}$ = 6.9 Hz, 12 H, CHMeMe), 1.16 (d, $^3J_{\text{H,H}}$ = 6.9 Hz, 12 H, CHMeMe) ppm. ^{13}C NMR (75 MHz, CDCl_3 , 293 K): δ = 166.0 (N=C), 156.5 (Py- C_o), 146.0 (Ar- C_{ip}), 145.4 (Py- C_{-Cl}), 135.7 (Ar- C_o), 123.8 (Ar- C_p), 123.0 (Py- C_m), 122.2 (Ar- C_m), 28.3 (N=C-Me), 23.3 (CHMeMe), 22.9 (CHMeMe), 17.2 (CHMe₂) ppm. IR: $\tilde{\nu}$ = 1640, 1557, 1317, 1260, 1228, 1189, 1104, 1016, 935, 885, 828, 762, 722, 692, 535, 438 cm⁻¹. $\text{C}_{33}\text{H}_{42}\text{ClN}_3$ (516.16): calcd. C 76.79, N 8.14, H 8.20; found C 73.23, N 7.21, H 8.35.

2,6-Bis[1-(2,6-dimethylcyclohexylimino)ethyl]pyridine (2all-cis): 2,6-Diacetylpyridine (2 g, 12.3 mmol), 2,6-dimethylcyclohexylamine all-*cis* (3.2 g, 25 mmol), and a few drops of acetic acid were poured into a three-necked round-bottomed flask containing ethanol (50 mL). The solution was refluxed for 18 h. After lowering the temperature, a white precipitate appeared. After filtration, washing with pentane and drying, a white solid was recovered (3.7 g, yield 82%). ^1H NMR (300 MHz, CDCl_3 , 293 K): δ = 8.18 (d, $^3J_{\text{H,H}}$ = 7.6 Hz, 2 H, py- H_m), 7.68 (t, $^3J_{\text{H,H}}$ = 7.6 Hz, 1 H, py- H_p), 3.71 (t, $^3J_{\text{H,H}}$ = 2.2 Hz, 2 H, CH_{cHex}-N=), 2.38 (s, 6 H, N=C-CH₃), 1.88–1.32 (br. m, 16 H, cHex-CH₂-), 0.70 (d, $^3J_{\text{H,H}}$ = 6.6 Hz, 12 H, cHex-CH₃) ppm. ^{13}C NMR (75 MHz, CDCl_3 , 293 K): δ = 164.0 (-C=N), 156.5 (py- C_o), 135.9 (py- C_p), 120.8 (py- C_m), 65.2 (CH_{cHex}-N=), 38.6 (cHex- C_o), 28.9 (cHex- C_m), 27.1 (cHex- C_p), 19.3 (cHex-CH₃),

13.3 (CH₃-C=N) ppm. IR: $\tilde{\nu}$ = 1703, 1638, 1567, 1303, 1237, 1156, 1116, 1086, 995, 980, 950, 857, 838, 818, 626, 558, 530, 491, 440, 338, 277 cm⁻¹. C₂₅H₃₉N₃ (381.60): calcd. C 78.69, N 11.01, H 10.30; found C 78.70, N 11.11, H 10.34.

2,6-Bis[1-(2,6-dimethylcyclohexylimino)ethyl]pyridine (2all-trans): 2,6-Diacetylpyridine (2 g, 12.3 mmol), 2,6-dimethylcyclohexylamine all-*trans* (3.2 g, 25 mmol), and a few drops of acetic acid were poured into a three-necked round-bottomed flask containing ethanol (50 mL). The solution was refluxed for 18 h. After lowering the temperature, a white precipitate appeared. After filtration, washing with pentane and drying, a white solid was recovered (3.6 g, yield 76%). ¹H NMR (300 MHz, CDCl₃, 293 K): δ = 8.09 (d, ³J_{H,H} = 7.7 Hz, 2 H, py-H_m), 7.69 (t, ³J_{H,H} = 7.7 Hz, 1 H, py-H_p), 2.92 (t, ³J_{H,H} = 9.3 Hz, 2 H, CH_{cHex}-N=), 2.39 (s, 6 H, N=C Me), 1.82–1.10 (br. m, 16 H, cyclohexyl -CH₂-), 0.74 (d, ³J_{H,H} = 6.6 Hz, 12 H, cHex-CH₃) ppm. ¹³C NMR (75 MHz, CDCl₃, 293 K): δ = 164.8 (-C=N), 156.8 (py-C_o), 136.5 (py-C_p), 121.0 (py-C_m), 72.8 (CH_{hex}-N=), 37.9 (cHex-C_o), 33.9 (cHex-C_m), 25.8 (cHex-C_p), 19.5 (cHex-CH₃), 14.7 (CH₃-C=N) ppm. IR: $\tilde{\nu}$ = 1643, 1567, 1305, 1237, 1172, 1153, 1116, 1088, 993, 948, 858, 839, 817, 779, 624, 555, 440, 340, 274, 228 cm⁻¹. C₂₅H₃₉N₃ (381.60): calcd. C 78.69, N 11.01, H 10.30; found C 78.45, N 11.41, H 10.38.

Synthesis of the Complexes

{4-Chloro-2,6-bis[1-(2,6-diisopropylphenylimino)ethyl]pyridine}iron Dichloride (1a): FeCl₂ (36 mg, 0.28 mmol) and 4-chloro-2,6-bis[1-(2,6-diisopropylphenylimino)ethyl]pyridine (150 mg, 0.29 mmol) were dissolved in THF (25 mL). The reaction was let run for 16 h. After precipitation with hexane, filtration, and drying, a blue powder was recovered (150 mg, yield 83%). ¹H NMR (300 MHz, CDCl₃, 293 K, $\delta_{\text{solvent}} = 7.26$): δ = 76.46 (s, 2 H, H_m, Py), 14.40 (s, 4 H, H_m Ar), -5.86 (br. s, 12 H, CHMeMe), -6.62 (s, 12 H, CHMeMe), -10.87 (s, 2 H, H_p Ar), -23.70 (br. s, 4 H, CHMe),

-45.57 (s, 6 H, NCMe) ppm. C₃₃H₄₂Cl₃FeN₃ (642.91): calcd. C 61.65, N 6.54, H 6.58; found C 61.88, N 6.01, H 7.35. IR: $\tilde{\nu}$ = 1689, 1574, 1500, 1320, 1282, 1237, 1115, 1015, 806, 722, 525, 365, 313 cm⁻¹.

{4-Chloro-2,6-bis[1-(2,6-diisopropylphenylimino)ethyl]pyridine}cobalt Dichloride (1b): CoCl₂ (38 mg, 0.29 mmol) and 4-chloro-2,6-bis[1-(2,6-diisopropylphenylimino)ethyl]pyridine (150 mg, 0.29 mmol) were dissolved in THF (25 mL). The reaction was let run for 16 h. After precipitation with hexane, filtration, and drying, a green powder was recovered (150 mg, yield 81%). C₃₃H₄₂Cl₃CoN₃ (646.00): calcd. C 61.36, N 6.50, H 6.55; found C 59.52, N 5.42, H 6.70. IR: $\tilde{\nu}$ = 1582, 1325, 1264, 1204, 1103, 1057, 1028, 938, 858, 854, 838, 798, 768, 722, 590, 487, 440, 347, 309, 280, 213 cm⁻¹.

{2,6-Bis[1-(2,6-dimethylcyclohexylimino)ethyl]pyridine}iron Dichloride (2a): FeCl₂ (132 mg, 1.04 mmol) and 2,6-bis[1-(2,6-dimethylcyclohexylimino)ethyl]pyridine all-*trans* (400 mg, 1.04 mmol) were dissolved in THF (25 mL). The reaction was let run for 16 h. After precipitation with hexane, filtration, and drying, a blue powder was recovered (400 mg, yield 75%). ¹H NMR (300 MHz, CD₂Cl₂, 298 K, $\delta_{\text{solvent}} = 5.32$): δ = 78.34 (s, 2 H, py-H_m), 10.14 (v br. s, 2 H, C_{cHex}-H), 8.84 (s, 2 H, C_{cHex}-H), 8.58 (s, 1 H, py-H_p), 3.46 (s, 2 H, C_{cHex}-H), 1.73 (s, 4 H, C_{cHex}-H), 1.02 (s, 4 H, C_{cHex}-H), -1.29 (s, 6 H, N=C-CH₃), -6.99 (br. s, 12 H, C_{cHex}-CH₃) ppm. C₂₅H₃₉Cl₂FeN₃ (508.35): calcd. C 59.07, N 8.27, H 7.73; found C 58.52, N 8.40, H 7.71. IR: $\tilde{\nu}$ = 1582, 1268, 1198, 1020, 948, 842, 816, 718, 639, 568, 314, 285 cm⁻¹.

{2,6-Bis[1-(2,6-dimethylcyclohexylimino)ethyl]pyridine}cobalt Dichloride (2b): CoCl₂ (136 mg, 1.04 mmol) and 2,6-bis[1-(2,6-dimethylcyclohexylimino)ethyl] all-*trans* (400 mg, 1.04 mmol) were dissolved in THF (25 mL). The reaction was let run for 16 h. After precipitation with hexane, filtration, and drying, a green powder

Table 3. Crystal data and structure refinement.

	1a	2a all-trans	2all-cis
Empirical formula	C ₃₇ H ₅₂ Cl ₃ FeN ₃ O C ₃₃ H ₄₂ Cl ₃ FeN ₃ ·C ₄ H ₁₀ O	C ₁₁₂ H ₁₈₂ Cl ₈ Fe ₄ N ₁₂ O ₄ C ₁₀₀ H ₁₅₆ Cl ₈ Fe ₄ N ₁₂ ·3C ₄ H ₈ O·H ₂ O	C ₂₅ H ₃₉ N ₃
Formula mass	717.05	2267.8(1)	381.59
Temperature [K]	173	173	173
Z	4	4	8
Crystal system	monoclinic	monoclinic	orthorhombic
Space group	P21/c	C2/c	Pbcn
a [Å]	10.3742(2)	43.5402(5)	23.0750(6)
b [Å]	20.2225(5)	12.5601(2)	14.6860(6)
c [Å]	18.6578(4)	26.2792(3)	13.7930(9)
β [°]	97.982(5)	117.157(5)	90.00
V [Å ³]	3876.3(1)	12787.0(6)	4674.2(4)
Color	blue	violet	colorless
Crystal size [mm]	0.20 × 0.06 × 0.02	0.16 × 0.12 × 0.06	0.20 × 0.20 × 0.15
D _{calcd.} [g·cm ⁻³]	1.23	1.17	1.085
F(000)	1520	4800	1680
Absorption coefficient [mm ⁻¹]	0.627	0.661	0.063
Index ranges	-14 ≤ h ≤ 14 -26 ≤ k ≤ 28 -26 ≤ l ≤ 26	0 ≤ h ≤ 61 0 ≤ k ≤ 17 -36 ≤ l ≤ 62	-29 ≤ h ≤ 29 -19 ≤ k ≤ 19 -17 ≤ l ≤ 17
θ range [°]	2.5–30.55	2.5–30.01	1.77–27.48
Reflections collected	12118	19449	5354
Reflections observed [I > 3 σ (I)]	3120	10571	2862
Number of parameters	406	632	253
R	0.046	0.076	0.0555
R _w	0.061	0.094	0.1278
Goodness-of-fit on F ²	1.028	1.119	0.954
Largest difference peak, hole [e·Å ⁻³]	0.350, -0.122	0.868, -0.873	0.183, -0.186

was recovered (350 mg, yield 65%). ^1H NMR (300 MHz, CDCl_3 , 293 K, $\delta_{\text{H}} = 7.26$): $\delta = 164.79$ (s, 2 H, $\text{C}_{\text{cHex}}\text{-H}$), 103.50 (s, 2 H, py-H_m), 27.73 (s, 1 H, py-H_p), 18.21 (s, 2 H, $\text{C}_{\text{cHex}}\text{-H}$), 3.70 (s, 2 H, $\text{C}_{\text{cHex}}\text{-H}$), 0.79 (s, 2 H, $\text{C}_{\text{cHex}}\text{-H}$), -4.72 (s, 4 H, $\text{C}_{\text{cHex}}\text{-H}$), -11.59 (s, 6 H, $\text{N}=\text{C-CH}_3$), -15.58 (s, 4 H, $\text{C}_{\text{cHex}}\text{-H}$), -16.02 [s (v br. sh), 2 H, $\text{C}_{\text{cHex}}\text{-H}$], -39.19 (s, 12 H, $\text{C}_{\text{cHex}}\text{-CH}_3$) ppm. $\text{C}_{25}\text{H}_{39}\text{Cl}_2\text{CoN}_3$ (511.44): calcd. C 58.71, N 8.20, H 7.69; found C 58.41, N 8.49, H 7.69. IR: $\tilde{\nu} = 1620, 1582, 1266, 1248, 1198, 1115, 1023, 948, 864, 823, 816, 746, 716, 638, 568, 317, 287\text{ cm}^{-1}$.

Polymerization Procedure: Polymerizations were conducted in a 250-mL glass Büchi reactor equipped with a magnetic stirrer and a temperature controller. Ethylene pressure was maintained constant in the reactor during the reaction. A typical procedure was: catalyst (10 μmol) in solution in toluene (30 mL) was added to the reactor under nitrogen. The reactor was heated to the reaction temperature and charged with ethylene. A solution of the desired amount of MAO dissolved in toluene (10 mL) was then added to the system. The reactor was charged with the desired differential pressure of ethylene. The reaction was let run for a period of 15 min, after which acidified ethanol (20 mL) was added to the miniclave to stop the polymerization. The content of the reactor was then precipitated in ethanol. The precipitated polymer was washed with ethanol and dried overnight in a vacuum oven at 60 °C.

X-ray Crystallography: Crystals of **1a**, **2a**, and **2all-cis** coated with vaseline were mounted onto the goniometer and placed on a Nonius Kappa CCD diffractometer with graphite-monochromated $\text{Mo-K}\alpha$ radiation ($\lambda = 0.71073\text{ \AA}$). The structures were solved using the Nonius OpenMoleN package and refined against F^2 using the SHELXL-97 software^[25] with anisotropic thermal parameters for all non-hydrogen atoms (except for one THF and the H_2O in **2a**) and hydrogen atoms were introduced as fixed contribution (SHELXL-97^[26]) (except for one THF and the H_2O in **2a**) (see Table 3).

CCDC-255729 (for $\text{C}_{33}\text{H}_{42}\text{Cl}_3\text{FeN}_3\cdot\text{C}_4\text{H}_{10}\text{O}$, **1a**), -255730 (for $\text{C}_{100}\text{H}_{156}\text{Cl}_8\text{Fe}_4\text{N}_{12}\cdot 3\text{OC}_4\text{H}_8\cdot\text{H}_2\text{O}$, **2a**), and -613556 (for $\text{C}_{25}\text{H}_{39}\text{N}_3$, **2all-cis**) contain the supplementary crystallographic data for this paper. These data can be obtained free of charge from The Cambridge Crystallographic Data Centre via www.ccdc.cam.ac.uk/data_request/cif.

Acknowledgments

The authors want to thank the CNRS for financial support, Prof. Richard Blackborow, BASF, and Dr. Rath for providing the 2,6-dimethylcyclohexylamines, Suzanne Zehnacker for DSC measurements, Emmanuel Ibarboure and Prof. Henri Cramail (LCPO, Bordeaux, France) for HT SEC measurements, Jean-Daniel Sauer for the low-temperature NMR measurements, Nathalie Kyritsakas-Gruber for X-ray refinements of the complexes, Dr. André De Cian for all the X-ray measurements and the X-ray refinement of the free ligand, and Dr. Marie-Thérèse Youinou for her helpful advice.

- [1] G. J. P. Britovsek, V. C. Gibson, B. S. Kimberley, P. J. Maddox, S. J. McTavish, G. A. Solan, A. J. P. White, D. J. Williams, *Chem. Commun.* **1998**, 849–850.
- [2] B. L. Small, M. Brookhart, A. M. A. Bennett, *J. Am. Chem. Soc.* **1998**, *120*, 4049–4050.
- [3] B. L. Small, M. Brookhart, *J. Am. Chem. Soc.* **1998**, *120*, 7143–7144.
- [4] a) G. J. P. Britovsek, M. Bruce, V. C. Gibson, B. S. Kimberley, P. J. Maddox, S. Mastroianni, S. J. McTavish, C. Redshaw, G. A. Solan, S. Strömberg, A. J. P. White, D. J. Williams, *J. Am. Chem. Soc.* **1999**, *121*, 8728–8740; b) V. C. Gibson, S. K. Spitzmesser, *Chem. Rev.* **2003**, *103*, 283–315.
- [5] J. Qiu, Y. Li, Y. Hu, *Polym. Int.* **2000**, *49*, 5–7.
- [6] G. J. P. Britovsek, S. Mastroianni, G. A. Solan, S. P. D. Baugh, C. Redshaw, V. C. Gibson, A. J. P. White, D. J. Williams, M. R. J. Elsegood, *Chem. Eur. J.* **2000**, *6*, 2221–2231.
- [7] Z. Ma, H. Wang, J. Qiu, D. Xu, Y. Hu, *Macromol. Rapid Commun.* **2001**, *22*, 1280–1283.
- [8] R. Chen, C. Qian, J. Sun, *Chin. J. Chem.* **2001**, *19*, 866–869.
- [9] A. S. Abu-Surrah, K. Lappalainen, U. Piironen, P. Lehmus, T. Repo, M. Leskelä, *J. Organomet. Chem.* **2002**, *648*, 55–61.
- [10] Z. Ma, W.-H. Sun, Z.-L. Li, C.-X. Shao, Y.-L. Hu, *Chin. J. Polym. Sci.* **2002**, *20*, 205–211.
- [11] Z. Ma, W.-H. Sun, N. Zhu, Z. Li, C. Shao, Y. Hu, *Polym. Int.* **2002**, *51*, 349–352.
- [12] R. Schmidt, U. Hammon, S. Gottfried, M. B. Welch, H. G. Alt, *J. Appl. Polym. Sci.* **2003**, *88*, 476–482.
- [13] Y. Chen, R. Chen, C. Qian, X. Dong, J. Sun, *Organometallics* **2003**, *22*, 4312–4321.
- [14] Y. Chen, C. Qian, J. Sun, *Organometallics* **2003**, *22*, 1231–1236.
- [15] H. Wang, W. D. Yan, T. Jiang, B. B. Liu, W. Q. Xu, J. J. Ma, Y. L. Hu, *Chin. Chem. Lett.* **2003**, *14*, 257–258.
- [16] M. E. Bluhm, C. Folli, M. Döring, *J. Mol. Catal. A* **2004**, *212*, 13–18.
- [17] a) F. Pelascini, F. Peruch, P. J. Lutz, M. Wesolek, J. Kress, *Eur. Polym. J.* **2005**, *41*, 1288–1295; b) V. C. Gibson, S. K. Spitzmesser, *Chem. Rev.* **2003**, *103*, 283–315; c) S. D. Ittel, L. K. Johnson, M. Brookhart, *Chem. Rev.* **2000**, *100*, 1169–1203; d) R. Mulhaupt, *Macromol. Chem. Phys.* **2003**, *204*, 289–327.
- [18] G. J. P. Britovsek, V. C. Gibson, S. Mastroianni, D. C. H. Oakes, C. Redshaw, G. A. Solan, A. J. P. White, D. J. Williams, *Eur. J. Inorg. Chem.* **2001**, 431–437.
- [19] G. J. P. Britovsek, V. C. Gibson, B. S. Kimberley, S. Mastroianni, C. Redshaw, G. A. Solan, A. J. P. White, D. J. Williams, *J. Chem. Soc., Dalton Trans.* **2001**, 1639–1644.
- [20] C. Amort, M. Malaun, A. Krajete, H. Kopacka, K. Wurst, M. Christ, D. Lilge, M. O. Kristen, B. Bildstein, *Appl. Organomet. Chem.* **2002**, *16*, 506–516.
- [21] C. Bianchini, G. Mantovani, A. Meli, F. Migliacci, F. Zanobini, F. Laschi, A. Scommazzi, *Eur. J. Inorg. Chem.* **2003**, 1620–1631.
- [22] G. J. P. Britovsek, V. C. Gibson, O. Hoarau, S. K. Spitzmesser, A. J. P. White, D. J. Williams, *Inorg. Chem.* **2003**, *42*, 3454–3465.
- [23] V. C. Gibson, S. K. Spitzmesser, A. J. P. White, D. J. Williams, *Dalton Trans.* **2003**, 2718–2727.
- [24] R. Ali Fallahpour, E. C. Constable, *J. Chem. Soc., Perkin Trans. 1* **1997**, 2263–2264.
- [25] A. M. A. Bennett, World Patent, WO9827124, **1998**.
- [26] G. M. Sheldrick, *SHELXL-97*, Program for the Refinement of Crystal Structures, University of Göttingen, Germany, **1997**.

Received: March 16, 2006

Published Online: August 24, 2006